Renewable Energy 83 (2015) 47–54

Contents lists available at ScienceDirect

Renewable Energy

journal homepage: www.elsevier.com/locate/renene

A general optimized geometry of angled ribs for enhancing the thermo-hydraulic behavior of a solar air heater channel – A Taguchi approach

Alireza Zamani Aghaie, Asghar B. Rahimi*, Alireza Akbarzadeh

Faculty of Engineering, Ferdowsi University of Mashhad, P.O. Box No. 91775-1111, Mashhad, Iran

ARTICLE INFO

Article history:
Received 6 December 2014
Accepted 6 April 2015
Available online

Keywords:
Angled-ribbed channel
Heat transfer
Friction factor
Thermal performance optimization
Taguchi method

ABSTRACT

The thermo-hydraulic behavior of the air flow through a solar air heater is numerically simulated and then optimized by use of Taguchi method. An innovative general geometry is introduced for the rib that variation in its parameters can generate triangular, trapezoidal and rectangular geometries simultaneously. A L_{16} (4^4) orthogonal array is used to optimize the geometry factors accounts for the maximum thermal performance of the ribbed channel. Thermal performance concept includes maximization of heat transfer coefficient and minimization of friction factor. Maximization of thermal enhancement factor is taken as the criteria of optimization. At a constant flow Reynolds number of 10,000, rib relative pitch (P/H), rib relative height (e/H), rib relative tip width (a/H) and rib front projection (s) are employed as the design factors. Results show that rib pitch, rib height, rib tip width and rib front projection have the greatest influences on the thermo-hydraulic performance, respectively. A triangular rib geometry with rib height of $0.2H$ and $P = 2H$ in which the rib front is normal to the flow direction (i.e. $s = 0$) is recognized as the optimum configuration.

1. Introduction

Since the fossil energy sources are decreasing rapidly, the energy matter has changed into one of the greatest concerns of the world. Therefore, employing new sources of energy (with an emphasis on renewable sources) and designing efficient energy systems are urgent needs of engineering fields. Solar energy is known to have a great potential among all other renewable sources of energy [1], and hence can be utilized as a source of power in many engineering applications. Solar air heaters are a type of heat exchangers which collect solar radiation to produces low to moderate temperatures (i.e. 30 °C–70 °C) [2]. Solar air heaters have various applications, such as local heating systems, solar water heaters, drying systems for agricultural products and dryer systems in civil engineering field. However, they usually have low thermal efficiency [3], which should be improved in order to make these systems more applicable and economical.

In order to achieve the maximum energy gain and enhance the heat transfer, different methods have been suggested. One the most convenient and effective techniques is using turbulator along the wall of the heat exchanger. The most regularly used turbulators in heat exchangers application are repeated winglets, grooves, ribs and artificially roughened surfaces. Turbulators enhance heat transfer by the following mechanisms:

- Increasing the effective area of heat transfer;
- Increasing the convective heat transfer coefficient, by creating turbulence through breaking the laminar sub-layer adjacent to wall.

However, this turbulence in the fluid flow would result in an increase of pressure drop, which is undesirable in heat exchanger application. Therefore, because of the twofold effects of turbulators, great considerations should be taken in modeling and designing such structures.

Numerous experimental and numerical researches have been carried out in design and optimization of heat exchangers with turbulators. Prasad and Saini [4,5] investigated the roughness

* Corresponding author.
E-mail address: rahimiab@yahoo.com (A.B. Rahimi).

http://dx.doi.org/10.1016/j.renene.2015.04.016
0960-1481/

geometry effects such as relative height and pitch on convective heat transfer and friction factor of fully developed turbulent flow in a solar air heater. They figured out that heat transfer reached its maximum amount near the reattachment points. They also found that for the case of relative roughness pitch to height ratio smaller than 8–10, reattachment of free shear layer was not formed. They achieved an enhancement of 2.38 and 4.25 times a smooth duct in heat transfer and friction factor, respectively. Karwa et al. [6] experimentally studied the thermo-hydraulic performance of air flow through a rectangular duct with repeated chamfered ribs mounted on one side and five different aspect ratios. The parameters under investigations were Reynolds number, relative roughness height, relative roughness pitch and rib chamfer angle. Based on their experiments, they proposed empirical correlations for heart transfer coefficient and friction factor. Bhagoria et al. [7] experimentally found correlations for heat transfer coefficient and friction factor in a rectangular solar air heater duct, which was equipped with transverse wedge shaped rib roughness on the absorber plate. These correlations described Nusselt number and friction factor in terms of rib geometry parameters and flow Reynolds number. A statistical approach, namely regression analysis, was applied to develop the correlations. Kenan Yakut et al. [8] optimized the design parameters of a heat exchanger having hexagonal fins, by use of Taguchi method. Kim et al. [9] optimized the design of an angled rib turbulator in a cooling channel by use of advanced response surface method with functional variables. In this work, rib angle of attack and pitch-to-rib height ratio were employed as the design parameters. Optimization was implemented in regard to maximum average heat transfer coefficient and maximum thermal enhancement factor. In 2010, Zeng et al. carried out a similar work for a heat exchanger with circular vortex-generator [10]. The design factors were attack angle, length of vortex generator, height of vortex generator, fin material, fin thickness, fin pitch and tube pitch on fin performance of vortex-generator fin-and-tube heat exchanger. Taguchi-based optimization of a tube with coiled-wire inserts was studied by Sibel Gunes et al. [11]. The effects of four design parameters, including ratio of the distance between the coiled wire and test tube wall to tube diameter, pitch ratio, ratio of the side length of equilateral triangle to tube diameter and Reynolds number, on heat transfer and pressure drop were investigated by using Taguchi method. Taguchi analysis was performed to reach maximum Nusselt number and minimum friction factor separately and then together. Isak Kotcioglu et al. [12] experimentally investigated a rectangular duct with plate-fins heat exchanger by applying Taguchi method in order to optimize the design geometry parameters. Pawar et al. [13] experimentally investigated heat transfer enhancement in a solar air heater with diamond shape ribs in its absorber plate. Influencing parameters, including rib relative height and pitch, Reynolds number and angle of attack were taken in to consideration. Kumar et al. [14] also applied a similar research on a rectangular duct having repeated V-shaped ribs with gap roughness on one broad wall. Their results showed that Nusselt number enhanced 6.74 times the smooth channel corresponding value, while fraction factor also increased by 6.37 times the smooth channel value. Based on the experimental results, empirical correlations were developed for *Nu* and friction factor as a function of roughness parameters and flow Reynolds number. Boulemtafes and Benzaoui [2] carried out a CFD numerical investigation on heat transfer enhancement in a solar air heater with transverse rectangular ribs. Four turbulence models, namely RNG k–ε, realizable k–ε, standard k–ω and SST k–ω were used in simulations in order to evaluate the performance of the models. A comprehensive review on thermo-hydraulic behavior of roughened surface solar air heaters can be found in Refs. [1,15–17].

In the current work, the thermo-hydraulic behavior of a periodic angled-ribbed channel with generalized rib geometry (Fig. 1) is investigated. This innovative geometry can generate any triangular, rectangular and trapezoidal ribs. Heat transfer coefficient (Nu), friction factor (f) and the thermal enhancement factor (η) are numerically calculated. The introduced general rib geometry is then optimized by Taguchi method and order of the factor with the most effect on thermal enhancement factor is determined.

2. Geometric modeling

The general configuration of the problem under investigation is illustrated in Fig. 1. In order to have a real case of study, the configuration of Boulemtafes-Boukadoum and Benzouri is used in this paper [2]. An air flow of $Re_D = 10{,}000$ (Reynolds number with regard to channel hydraulic diameter) is passed through the channel of height $H = 40$ mm. This air flow is provided with a ventilator which implies a forced convective heat transfer inside the channel. The channel outlet is set to have the atmospheric temperature. The upper wall of the channel is assumed to be adiabatic, while the lower ribbed surface exposed to a constant heat flux of 4000 W/m^2 (this flux is imposed to the whole surface including the tilted one). The factors affect the general introduced geometry are the height of the rib (e), ribs pitch (i.e. the distance between two adjacent ribs) (P), rib tip width (a) and rib front projection distance (s) with a constant rib total width of $W = H = 40$ mm. It is recognized that the cases of ($a/H = 0$) and ($a/H = 1$ & $s = 0$) correspond to triangular and rectangular ribs, respectively, while other values of $0 < a/H < 1$ stand for trapezoidal rib. All these cases are known as common and applicable rib geometries used in industries. Furthermore, getting different values by s (from 0% to 100% of rib front projection distance, i.e. (H − a)) produces various cases of rib front position against the flow. The case $s = 0$ corresponds to the condition in which the rib front is normal to the flow direction. Due to the importance of recirculation zone behind the ribs, i.e. the gap between two adjacent ribs, pitch distance (P) is also assigned to get different values. When P/H is set to be 1, it generates the case of no gap (recirculation zone) between the ribs.

The computational domain is extended 8 times of the channel hydraulic diameter ($D_h = 2H = 80$ mm) for the upstream section to ensure a uniform inlet flow and 12 times for the downstream section in order to prevent any recirculation at the outlet, i.e. preserve fully developed condition [18]. Because the thermo-hydraulic behavior of a ribbed surface is recognized to be independent of the number of ribs when it exceeds 6 [10], seven ribs are considered along the test section of the channel.

3. Mathematical modeling

The thermo-hydraulic behavior of the averaged fluid flow quantities in forced convective heat transfer mode is mathematically described by the continuity, momentum and energy equations. The steady state form of these equations can be written in Cartesian system as:

Continuity equation [19]:

$$\frac{\partial}{\partial x_i}(\rho u_i) = 0 \tag{1}$$

Momentum equation [19]:

$$\frac{\partial}{\partial x_j}(\rho u_i u_j) = -\frac{\partial P}{\partial x_i} + \frac{\partial}{\partial x_j}\left[\mu\left(\frac{\partial u_i}{\partial x_j} + \frac{\partial u_j}{\partial x_i}\right) - \rho\overline{u_i' u_j'}\right] \tag{2}$$

Energy equation [19]:

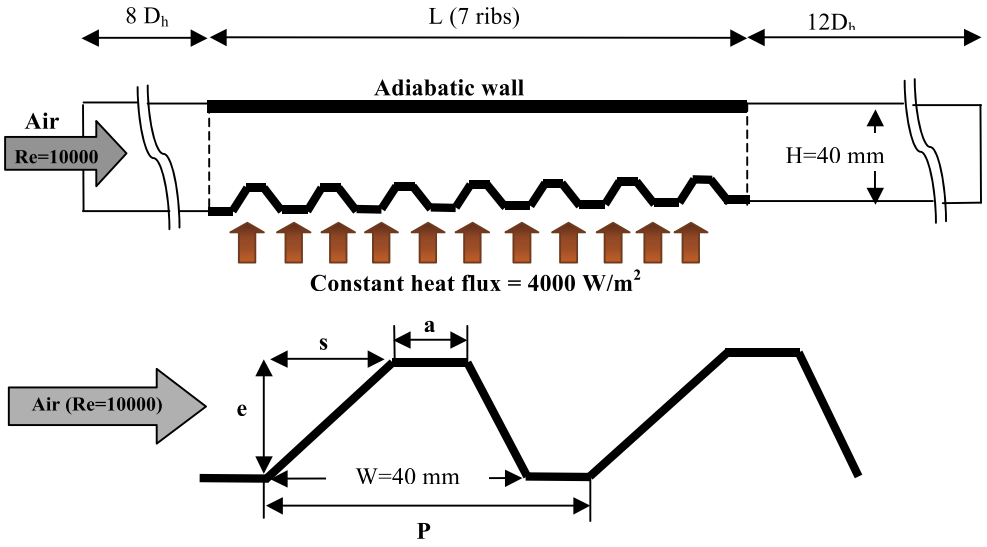

Fig. 1. General geometry of the ribbed channel under investigation.

$$\frac{\partial}{\partial x_j}(\rho u_j T) = \frac{\partial}{\partial x_j}\left[(\Gamma + \Gamma_t)\frac{\partial T}{\partial x_j}\right] \tag{3}$$

In the above equations, x_i is the coordinate system component, u_i is the flow velocity component and ρ, P, μ and T are flow density, pressure, viscosity coefficient and temperature, respectively. In Eq. (3), Γ and Γ_t are molecular thermal diffusivity and turbulent thermal diffusivity, respectively and are given by

$$\Gamma = \frac{\mu}{\mathrm{Pr}} \quad \text{and} \quad \Gamma_t = \frac{\mu_t}{Pr_t} \tag{4}$$

where Pr is Prandtl number and subscript t stands for turbulent properties. The term $-\overline{\rho u_i u_j}$ in Eq. (2) is the Reynolds stress tensor which represents the mean flux of momentum due to the turbulent fluctuations and should be modeled. For this purpose, RNG k-ε model is employed in the current work. The Reynolds stress tensor can be related to the mean flow velocities by Boussinesq relation as [19]:

$$-\overline{\rho u_i u_j} = \mu_t\left(\frac{\partial u_i}{\partial x_j} + \frac{\partial u_j}{\partial x_i}\right) \tag{5}$$

4. Numerical method

4.1. Geometry and computational grid

The two dimensional ribbed horizontal channel is illustrated with all the geometrical parameters in Fig. 1. The rib geometry is designed in a way that produces either the triangular rib geometry ($a = 0$), trapezoidal rib ($0 < a < H$) and rectangular rib ($a = H$) geometries, which are known as three of the most famous and convenient ribs in industry. Therefore, it makes it possible to decide about the optimum rib geometry between a triangular rib, rectangular rib and an unstructured angled-rib geometries.

A uniform rectangular mesh with grid adoption for dimensionless wall distance of $y^+ \approx 2$ at an adjacent wall region was used [20], while a finer mesh was generated close to the walls and ribs to resolve the rapidly changing flow structures in those regions, and hence reach efficient numerical solution and save the computational time. Generating the computational grid was done by the preprocessor GAMBIT 2.3.16 software [21]. The mesh independency study has been carried out which is shown in Fig. 2. In this figure, local Nusselt number is plotted on one side of the last rib. A mesh grid with a total cells number of 190,750 was found to be suitable for the numerical solution which satisfied the grid independency of the results.

4.2. Solution procedure

The commercial CFD software FLUENT 6.3.26 was used for numerically solving the governing equations [22]. The second order upwind differencing scheme was applied to the convective and turbulent terms, and also the energy equation. QUICK differencing scheme was used for momentum equation solution [22]. The diffusion terms were discretized by the second order central differencing scheme. To evaluate the pressure field, SIMPLE (Semi Implicit Method for Pressure Linked Equation) algorithm was used for coupling the pressure and velocity terms [22]. The boundary conditions applied to the case under consideration is tabulated in.

In Eqs. (9) and (10), the subscript s stands for the smooth channel of hydraulic diameter D_h.

Table 1. As prescribed by Kim et al. [9], RNG k–ε turbulence model was employed in simulations.

The average Nusselt number, Nu, is the dimensionless parameter used for assessing the heat transfer enhancement and defined as [19]:

$$Nu = \frac{1}{L}\int \frac{h(x)\cdot D_h}{k}dx \tag{6}$$

where $h(x)$ is the local convective heat transfer coefficient, k is the thermal conductivity and D_h is the hydraulic diameter of the channel (here, $D_h = 2H$). The friction factor, f, is the parameter accounts for the pressure drop along the channel. The friction factor over a test section of length L with a pressure drop of ΔP and flow average velocity of u is calculated by [19]:

$$f = \frac{\Delta P\cdot D_h}{\frac{1}{2}\rho u^2 L} \tag{7}$$

In order to investigate the twofold effect of turbulence on thermo-hydraulic behavior of the flow, namely enhancing the heat

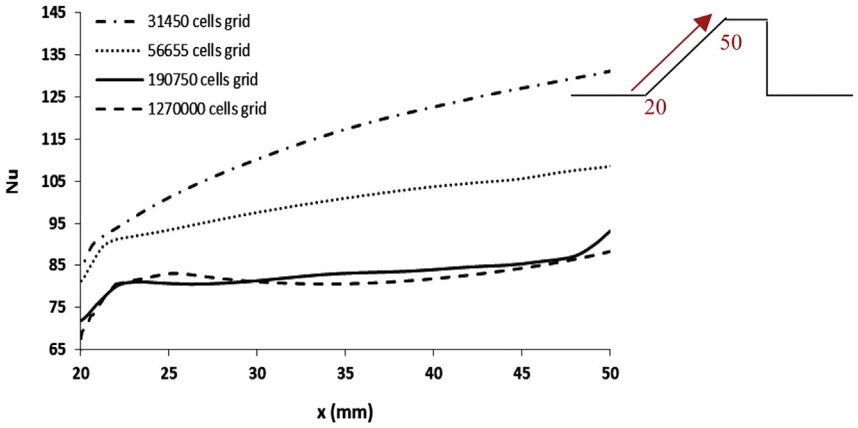

Fig. 2. Grid independency study for different total number of cells – local Nusselt number variation along the shown side of the last rib.

Table 1
-Boundary condition.

Fluid	Air at standard atmospheric condition
Inlet	Velocity inlet with Re = 10,000 and 5% turbulence intensity
Outlet	Pressure outlet with ambient pressure and 5% turbulence intensity
Upper wall	Adiabatic wall
Lower wall	Constant heat flux at the test section (4000 W/m^2) & no slip

transfer and increasing the pressure drop, thermal enhancement factor is introduced as [19]:

$$\eta = \frac{(Nu/Nu_s)}{(f/f_s)^{1/3}} \tag{8}$$

where subscript s represents the smooth channel properties.

Modified Blasius and Dittus–Boethler correlations [23] are presented for determining the friction factor and Nusselt number in a smooth heated channel, respectively, as:

$$f_s = 0.085\, Re^{-0.25} \tag{9}$$

$$Nu_s = 0.024\, Re^{0.8} Pr^{0.4} \tag{10}$$

In Eqs. (9) and (10), the subscript s stands for the smooth channel of hydraulic diameter D_h.

5. Taguchi method

Taguchi method is known as one the widely-used tools in engineering applications, which helps optimizing the engineering experiments through determination of best choices of factors influenced on a physical phenomenon, with the minimum number of experiments [24,25]. Therefore, requiring the minimum amount of experiments makes this engineering optimization tools an efficient one. In order to cover a full representation of full-factorial experiment, Taguchi method employs some standard tables of experiments, called orthogonal arrays [26]. These orthogonal arrays prescribe specific arrangement of fractional experiments with regard to the influencing factors and their levels. In the current work, a L_{16} (4^4) orthogonal array was used, which implied carrying out 16 tests with 4 factors of 4 levels that listed in Table 2.

After implementing the numerical simulations, based on the prescribed Taguchi orthogonal array of Table 2, the results are transformed into signal-to-noise ratio (SNR). Signal and noise stand for controllable and uncontrollable factors in a physical phenomenon, respectively [11]. Signals in this paper are listed in the first column of Table 2, where the noise is thermal enhancement factor. SNR is a tool in Taguchi method that helps measuring the performance variability. According to Taguchi method, the optimum condition corresponds to case where the noise factors implies the minimum variation of the system performance [12]. In other words, the case of the highest SNR represents the optimum configuration of the system. Quality characteristic in the analysis of SNR categorized into three cases, namely the-higher-the-better, the-lower-the-better and the-nominal-the-better [11]. Here, the aim of optimization is to maximize the thermal enhancement factor (η), i.e. the case of the-higher-the-better. SNR in the current work is defined as [10]:

Table 2
Taguchi factors and levels [26].

Factors		Levels			
		1	2	3	4
1	Rib relative pitch (P/H)	1	1.3	1.7	2
2	Rib relative height (e/H)	0.05	0.2	0.5	0.75
3	Rib relative tip width (a/H)	0	0.3	0.6	1
4	Rib relative front projection (s/(H – a))	0	0.25	0.6	1

$$SNR = -10 \log\left(\frac{1}{N}\sum_{i=1}^{N}\eta_i^2\right) \tag{11}$$

Where N is the number of repetitions in confirmation experiments. Further explanations on Taguchi method can be found in Refs. [8,11,12,24–28].

6. Results and discussion

As shown in Fig. 3, the numerical solution of RNG k-ε turbulence model [23] with parameter e/H = 0 and Pr = 0.71 [29] is validated based on the correlations introduced in Eqs. (9) and (10).

The current numerical simulation is also applied to the channel of [30] and the result is compared to the experimental results (Fig. 4), as the other validation of the numerical code.

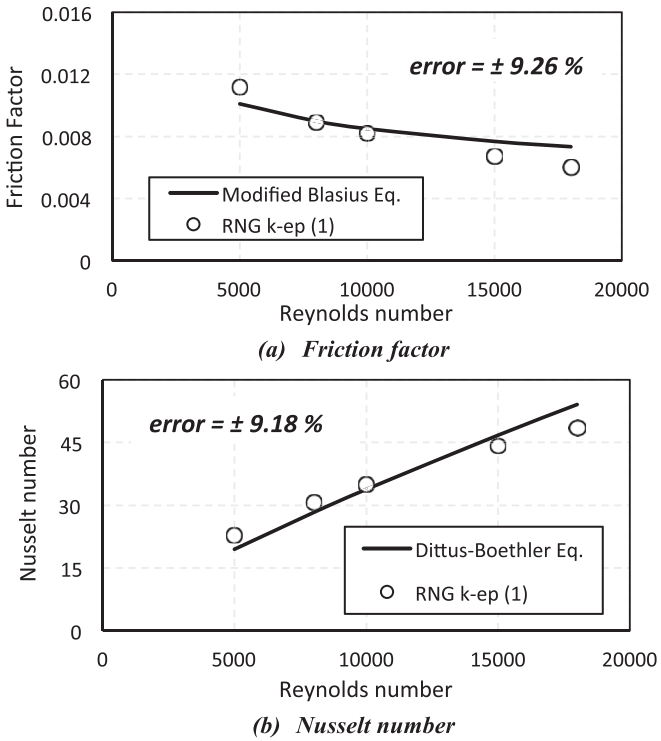

Fig. 3. Validation of numerical solution with exact results.

As seen from Fig. 4, there is a very good agreement between the numerical results and the experimental results of [30].

Assigned implementations with their corresponding results are presented at Table 3. It should be noted again that the cases of a/H = 1 corresponds to rectangular rib, which implies that s = 0.

Having applied the Taguchi analysis, the response table for Signal-to-Noise Ratios (SNR) in this case is given in Table 4 and plotted in Fig. 5. The importance of the factors on the thermal enhancement factor is ranked in the last row of the table. The factor with the higher difference between maximum and minimum values of SNR has the higher influence.

It is understood from Table 4 and Fig. 5 that rib relative pitch (P/H), rib height (e/H), rib tip width (a/H) and rib front projection ($s/(H-a)$) respectively have the most effect on thermal enhancement factor increase. From Fig. 5, it is recognized that the highest SNRs of rib relative height (e/H) and rib front relative projection ($s/(H-a)$) are not bold and the difference between the highest value and the next one is very small. Hence, in order to increase in accuracy of prediction, four cases, as listed in Table 5, were determined initially as the optimum configurations. These cases were then numerically solved and their thermal enhancement factors were compared to each other, in order to specify the final optimum configuration.

Based on the results shown in Table 5, the second case which is a triangular rib with upstream front perpendicular to the flow direction was found to be the optimized geometry for the angled rib. Fig. 6 shows the optimized rib geometry and the computational grid used for the numerical solution.

Table 3
Taguchi table – the implementations configuration and their corresponding results.

Test no.	Factors				Results		
	P/H	e/H	a/H	S/(H − a)	f	Nu	η
1	1	0.05	0	0	3.83E-03	29.65	1.14
2	1	0.2	0.3	0.25	4.46E-03	34.13	1.25
3	1	0.5	0.6	0.6	1.35E-02	44.2	1.12
4	1	0.75	1	1	8.50E-03	33.8	1.00
5	1.3	0.05	0.3	0.6	7.05E-03	33.73	1.06
6	1.3	0.2	0	1	6.66E-03	38.28	1.23
7	1.3	0.5	1	0	2.08E-02	53.1	1.17
8	1.3	0.75	0.6	0.25	5.07E-02	86.2	1.41
9	1.7	0.05	0.6	1	8.60E-03	41.08	1.21
10	1.7	0.2	1	0.6	8.50E-03	49.4	1.46
11	1.7	0.5	0	0.25	1.43E-02	74.5	1.85
12	1.7	0.75	0.3	0	5.40E-02	109	1.74
13	2	0.05	1	0.25	8.09E-03	47.19	1.42
14	2	0.2	0.6	0	5.60E-03	59.71	2.03
15	2	0.5	0.3	1	1.81E-02	70	1.61
16	2	0.75	0	0.6	5.95E-02	122.7	1.90

Table 4
Factorial effect for thermal enhancement factor.

	Level	Factors			
		P/H	e/H	a/H	$s/(H-a)$
SNR	1	1.03	1.60	3.47	3.37
	2	1.65	3.30	2.86	3.33
	3	3.78	2.95	2.94	2.59
	4	4.72	3.34	1.92	1.90
Delta (max−min)		3.69	1.74	1.55	1.47
Rank		1	2	3	4

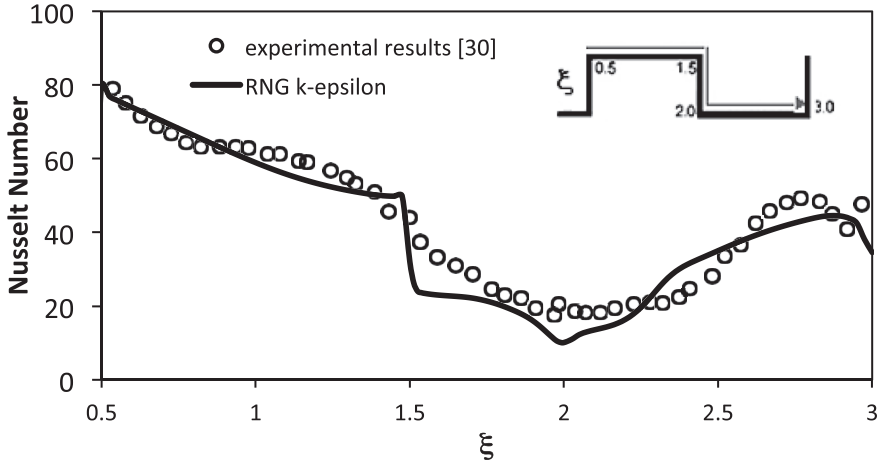

Fig. 4. Validation of numerical solution with experimental results of [30] – (H = 40 mm, W=H, P = 2H, e/H = 0.5 and a/H = 1).

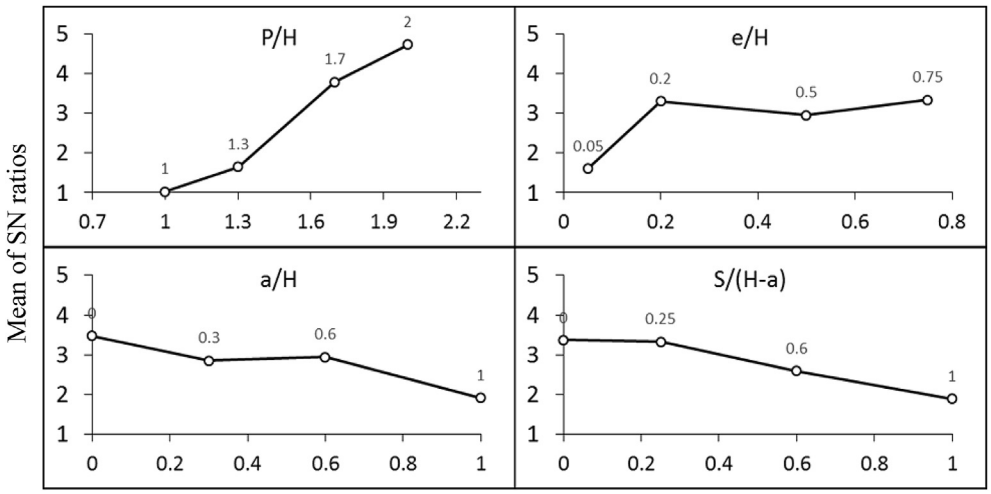

Fig. 5. Main effects plot for S/N ratios – thermal enhancement factor to be maximized (i.e. larger SNR is better).

Table 5
Probable optimum designs – maximizing the thermal enhancement factor.

	P/H	e/H	a/H	S/(H − a)	f	Nu	η
Case 1	Level 1 (2)	Level 4 (0.75)	Level 1 (0)	Level 1 (0)	6.90E-02	132.9	1.96
Case 2	**Level 1 (2)**	**Level 2 (0.2)**	**Level 1 (0)**	**Level 1 (0)**	**4.40E-03**	**62.66**	**2.31**
Case 3	Level 1 (2)	Level 4 (0.75)	Level 1 (0)	Level 2 (0.25)	6.50E-02	129	1.94
Case 4	Level 1 (2)	Level 2 (0.2)	Level 1 (0)	Level 2 (0.25)	5.60E-03	58	1.97

Separation, re-attachment and flow reversal can be easily noticed in velocity vectors of Fig. 7. All the simulations are implemented for air flow at $Re = 10{,}000$.

The influence priority of different factors can be discovered from Table 4. In this regard, the factors effects are individually illustrated in Fig. 8.

As previously found, relative pitch (P/H) has the most influence on thermal enhancement factor. Depending on the value of P/H, flow will experience different patterns, from a single vortex generation to separation, re-attachment and re-separation within the gap between the succeeding ribs. Fig. 8(a) reveals that the larger the gap (i.e. the higher the P/H value), the more the flow tends to the pattern of separation and multi vortex generation and thus, the higher the heat transfer rate is. However, these flow reversal cause a pressure drop along the channel, which results in decrease of thermal enhancement factors. But, because the rate of Nusselt number increase is greater than friction factor decrease, thermal enhancement factor will be increased by an increase in pitch. Making the flow more turbulent, rib height increase leads to increase of heat transfer coefficient (as seen in Fig. 8(b)), but it also yields an increase in friction factor. Whenever the rib height exceeds the viscous sub-layer and disturbs the flow filed in the core of the channel, the rate of increase in friction factor will be much greater than increase in Nusselt number. Thus, thermal enhancement factor increased by an increase in rib height until e/H ~ 0.25 and then decrease due to sever increase in friction factor. Rib top width and side projection were distinguished to have the lowest effect on the thermal enhancement factor. These factors influence on the thermo-hydraulic behavior through the mechanism of flow separation and reattachment and vortex generation. It is understood from Fig. 8(c) that wider the rib tip, the less the probability of vortex generation and flow separation, and hence the lower Nusselt number and higher friction factor.

7. Conclusion

The heat transfer coefficient, friction factor and thermal enhancement factor are numerically investigated and optimized by

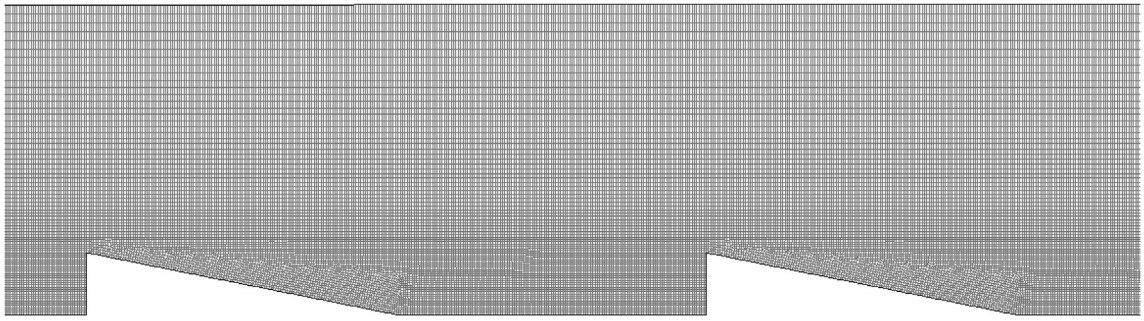

Fig. 6. Optimized geometry of angled rib, with P/H = 2, e/H = 0.2, a = 0 and s = 0.

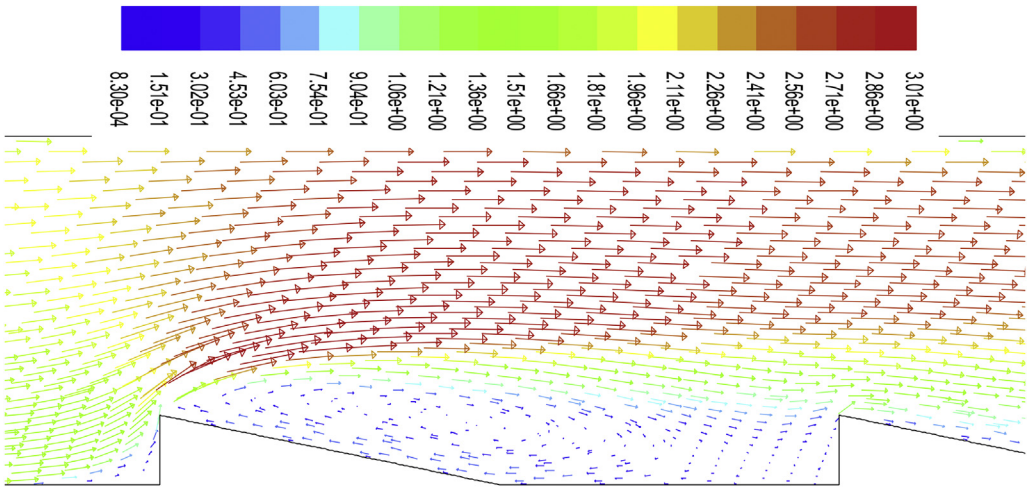

Fig. 7. Flow around the first two optimized ribs – colored velocity scale in m/s.

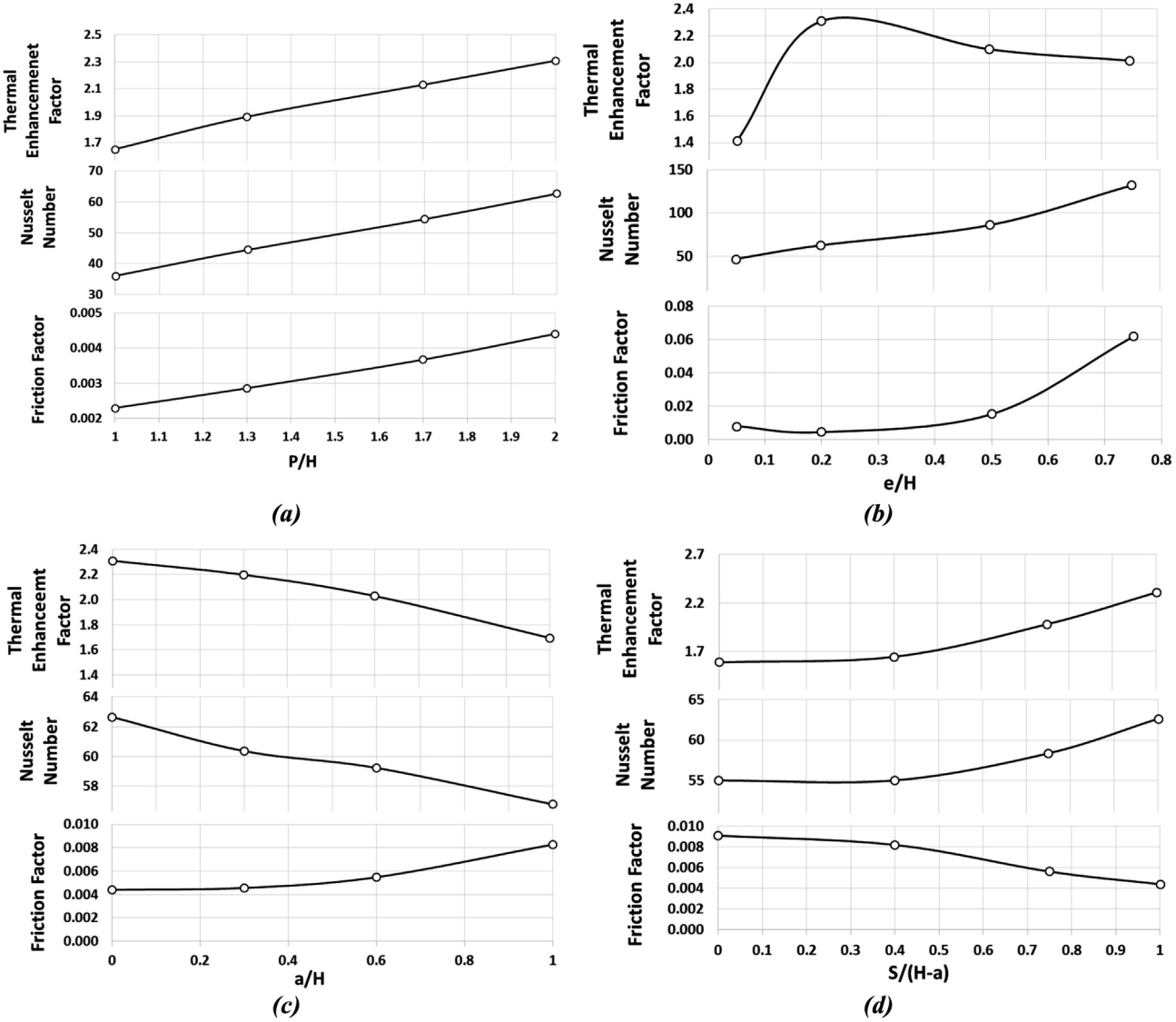

Fig. 8. Effects of different factors on thermo-hydraulic behavior: a) P/H effect (e/H = 0.2, a/H = 0 and s/(H − a) = 0) − b) e/H effect (P/H = 2, a/H = 0 and s/(H − a) = 0) − c) a/H effect (P/H = 2, e/H = 0.2 and s/(H − a) = 0) − d) s/(H − a) effect (P/H = 2, e/H = 0.2 and a/H = 0).

use of a $L_{16}(4^4)$ Taguchi orthogonal array test arrangement. In each investigation, average Nusselt number and friction factor over the ribbed surface are calculated and used to determine the thermal enhancement factor. This parameter is employed as the performance parameter in Taguchi analysis which is supposed to be maximized. Applying the Taguchi method the optimum rib geometry is obtained. Results reveal that rib relative pitch and relative height have the most impact on enhancing thermo-hydraulic behavior of a solar air heater with angled ribs, respectively. Having simulated the cases, the optimum configuration is determined to be a triangular rib with upstream front normal to the direction of the flow, i.e. $P/H = 2$, $e/H = 0.2$ and $a = s = 0$.

References

[1] Kumar A, Saini RP, Saini JS. A review of thermohydraulic performance of artificially roughened solar air heaters. Renew Sustain Energy Rev 9//2014;37:100–22.
[2] Boulemtafes-Boukadoum A, Benzaoui A. CFD based analysis of heat transfer enhancement in solar air heater provided with transverse rectangular ribs. Energy Procedia 2014;50:761–72.
[3] D JA, B WA. Solar engineering of thermal processes. NY: New York: Wiley Interscience publications; 1980.
[4] Prasad BN, Saini JS. Optimal thermohydraulic performance of artificially roughened solar air heaters. Sol Energy 1991;47:91–6.
[5] Prasad BN, Saini JS. Effect of artificial roughness on heat transfer and friction factor in a solar air heater. Sol Energy 1988;41:555–60.
[6] Karwa R, Solanki SC, Saini JS. Heat transfer coefficient and friction factor correlations for the transitional flow regime in rib-roughened rectangular ducts. Int J Heat Mass Transf 5/1/1999;42:1597–615.
[7] Bhagoria JL, Saini JS, Solanki SC. Heat transfer coefficient and friction factor correlations for rectangular solar air heater duct having transverse wedge shaped rib roughness on the absorber plate. Renew Energy 3//2002;25:341–69.
[8] Yakut K, Alemdaroglu N, Sahin B, Celik C. Optimum design-parameters of a heat exchanger having hexagonal fins. Appl Energy 2//2006;83:82–98.
[9] Kim K, Lee H, Kim B, Shin S, Lee D, Cho H. Optimal design of angled rib turbulators in a cooling channel. Heat Mass Transf 2009/10/01;45:1617–25.
[10] Zeng M, Tang LH, Lin M, Wang QW. Optimization of heat exchangers with vortex-generator fin by Taguchi method. Appl Therm Eng 9//2010;30:1775–83.
[11] Gunes S, Manay E, Senyigit E, Ozceyhan V. A Taguchi approach for optimization of design parameters in a tube with coiled wire inserts. Appl Therm Eng 10//2011;31:2568–77.
[12] Kotcioglu I, Cansiz A, Nasiri Khalaji M. Experimental investigation for optimization of design parameters in a rectangular duct with plate-fins heat exchanger by Taguchi method. Appl Therm Eng 1/10/2013;50:604–13.
[13] Pawar SS, Hindolia DA, Bhagoria JL. Experimental study of Nusselt number and friction factor in solar air heater duct with diamond shaped rib roughness on absorber plate. Am J Eng Res (AJER) 2013;2:60–8.
[14] Kumar A, Saini RP, Saini JS. Development of correlations for Nusselt number and friction factor for solar air heater with roughened duct having multi v-shaped with gap rib as artificial roughness. Renew Energy 10//2013;58:151–63.
[15] Hans VS, Saini RP, Saini JS. Performance of artificially roughened solar air heaters—a review. Renew Sustain Energy Rev 10//2009;13:1854–69.
[16] Alam T, Saini RP, Saini JS. Use of turbulators for heat transfer augmentation in an air duct – a review. Renew Energy 2//2014;62:689–715.
[17] Alam T, Saini RP, Saini JS. Heat and flow characteristics of air heater ducts provided with turbulators—a review. Renew Sustain Energy Rev 3//2014;31:289–304.
[18] Han JC, Park JS. Developing heat transfer in rectangular channels with rib turbulators. Int J Heat Mass Transf 1//1988;31:183–95.
[19] Eiamsa-ard S, Promvonge P. Numerical study on heat transfer of turbulent channel flow over periodic grooves. Int Commun Heat Mass Transf 8//2008;35:844–52.
[20] Schlichting H, Gersten K, Gersten K. Boundary-layer theory. Springer; 2000.
[21] GAMBIT 2.3-User's guide. Fluent Inc; 2006.
[22] FLUENT 6.3-User's guide. Fluent Inc; 2006.
[23] Bhatti MS, Shah RK. Turbulent and transitional flow convective heat transfer. In: Hand book of single-phase convection heat transfer. New York: John Wiley and Sons; 1987.
[24] Ross PJ. Taguchi techniques for quality engineering: loss function, orthogonal experiments, parameter and tolerance design. McGraw-Hill; 1996.
[25] Taguchi G. System of experimental design. New York: Quality Resources; 1987.
[26] Taguchi G, Konishi S. Orthogonal arrays and linear graphs: tools for quality engineering. Dearborn, Mich., USA: American Supplier Institute; 1987.
[27] Phadke MS. Quality engineering using robust design. Prentice Hall; 1989.
[28] Fei NC, Mehat NM, Kamaruddin S. Practical applications of Taguchi method for optimization of processing parameters for plastic injection moulding: a retrospective review. ISRN Ind Eng 2013;2013:11.
[29] Bergman TL, Incropera FP, Lavine AS. Fundamentals of heat and mass transfer. Wiley; 2011.
[30] Lorenz S, Mukomilow D, Leiner W. Distribution of the heat transfer coefficient in a channel with periodic transverse grooves. Exp Therm Fluid Sci 10//1995;11:234–42.